Real-Time Pipe Fault Detection System Using Computer Vision

Hyoung-Seok Kim[1], Byung-Ryong Lee[1,#]

1 School of Mech. & Auto. Engineering, University of Ulsan, Ulsan, South Korea
Corresponding Author / E-mail: brlee@ulsan.ac.kr, TEL: +82-52-259-2147, FAX: +82-52-259-1680

KEYWORDS : Hough transform, Pipe fault inspection, Data transform, Computer vision

Recently, there has been an increasing demand for computer-vision-based inspection and/or measurement system as a part of factory automation equipment. In general, it is almost impossible to check the fault of all parts, coming from part-feeding system, with only manual inspection because of time limitation. Therefore, most of manual inspection is applied to specific samples, not all coming parts, and manual inspection neither guarantee consistent measuring accuracy nor decrease working time. Thus, in order to improve the measuring speed and accuracy of the inspection, a computer-aided measuring and analysis method is highly needed.

In this paper, a computer-vision-based pipe inspection system is proposed, where the front and side-view profiles of three different kinds of pipes, coming from a forming line, are acquired by computer vision. And the edge detection is processed by using Laplace operator. To reduce the vision processing time, modified Hough transform is used with clustering method for straight line detection. And the center points and diameters of inner and outer circle are found to determine eccentricity of the parts. Also, an inspection system has been built so that the data and images of faulted parts are stored as files and transferred to the server.

Manuscript received: January 17, 2005 / Accepted: May 12, 2005

1. Introduction

Computer vision system, as a part of the factory automation, could be applied for quality inspection, classification, recognition, etc., instead of human vision.[1,2]

Recently, factory automation technology in manufacturing area has been growing rapidly, however inspection process, the last step of the manufacturing, remains at the low level of technology. Most of part-inspection processes still depend on human vision. Conventional human-vision based inspection causes many problems such as eye exhaustion, concentration decrease, inconsistent criterion, difficulty in fast feedback, and high labor costs, etc. One alternative method for the problems is to apply a computer vision system to factory automation. Since mid-1980's, vision inspection system using the CCD cameras has been studied and proved to have a lot of advantages with low cost and system simplicity.[3,4] Persoon[5] studied vision inspection system for IC chip fault detection, and Toshiyuki et. al.[6] developed an algorithm for book sorting system using the pattern matching. Shapiro et. al.[7] developed a failure inspection system for ALC blocks, which improved the measurement resolution from 0.05cm to 0.01cm. As stated above, with inspection system using CCD camera it needs to draw out the feature of the edge for the specific parts. The Hough transform among the feature detection methods has been developed to detect definable shapes (line, circle, ellipse etc.) analytically from the image data. The main advantage of the Hough transform is getting robustness against noise, however the method has a disadvantage of requiring large memory and the preliminary information of the shape for the exact partition.[8,9,10]

In this paper, A computer vision based system is developed to inspect the automotive oil pipes and discriminate whether the pipe is normal or abnormal. The inspection algorithm detects line segments from side-view image using Hough transform and finds pipe angle, eccentricity, and diameter. Using front-view image, the algorithm finds center points and diameters of inner/outer circles to determine the pipe fault status by applying a line-scanning method. Three types of pipes, *Φ10*, *Φ8*, and *Φ6.35mm* are tested by the inspection system. *Φ6.35mm* pipe has two types according to the end shapes of the pipes. The inspection algorithm finds the diameter of pipe and decides good or bad condition of the pipes. If a pipe is found to be faulty, the system saves the image itself as image file, and inner diameter, outer diameter, angle, and eccentricity as data files. In case of good pipe, the system saves the data such as inner and outer diameters as only text file. And then, two files (one file in case of good pipe) are sent to the sever computer. This system enables supervisor to handle all data through batch processing.

2. Pipe-fault-detection system

In this section an entire flow chart of vision inspection system and the inspection algorithm are introduced. Fig.1 shows the entire flowchart of the pipe inspection system using computer vision. Overall system consists of two inspection station. One station inspects the forming status of the left end of pipes, the other station inspects the forming status of the right end of pipes. If there exist any forming faults, the pipe is removed by an actuator.

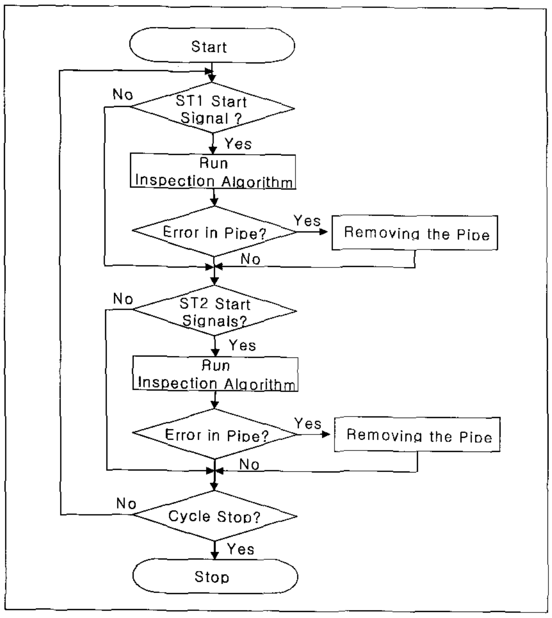

Fig. 1 Flowchart of the pipe-fault-detection system

Fig.2 shows the fault detection algorithm for different types of pipes. The side-view inspection algorithm extracts line segments and angles by using Hough transform and calculates the eccentricity and maximum diameter of the pipe. The front-view inspection algorithm calculates center points, inner and outer diameters of pipe by using a line-scanning method. Using both side-view and front-view inspection algorithms, the forming failure of pipes can be detected with a high accuracy.

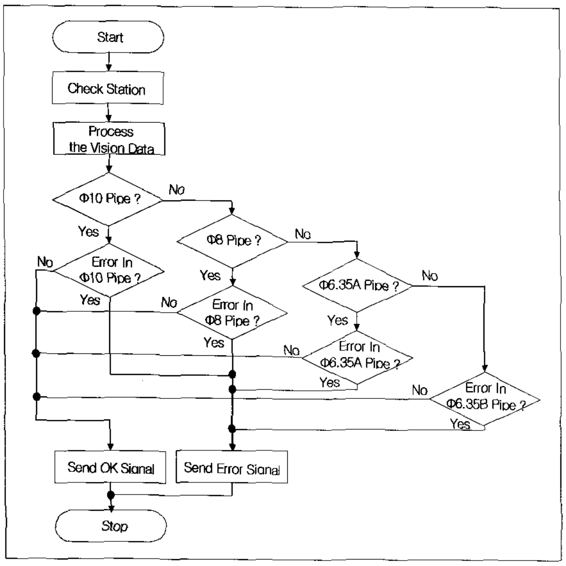

Fig. 2 Flowchart of the inspection algorithm

2.1 Side-view inspection algorithm

Considering a line $y = ax + b$, parameters a and b can have values in the range of $-\infty<a<\infty$ and $-\infty<b<\infty$. Therefore, it is difficult to express the line equation in the parametric space, and a lot of memory quantity is needed to store each line data. If the line $y = ax + b$ is represented as $\rho = x\cos\theta + y\sin\theta$ then the range of ρ and θ can be limited between $-N\sqrt{2} \le \rho \le N\sqrt{2}$ and $-\pi \le \theta \le \pi$. The quantity of memory and calculation difficulty can be efficiently reduced because of the limited space of the parameters. However, some additional treatment should be considered in order to reduce further the inspection time. For this purpose we use clustering structure, in which a subset area with relatively many points is found. The straight line equation obtained from a set of partial points may have some fuzzy distribution because of the noise effect of Hough transform. Therefore, the line equation needs to be approximated using the Gaussian function, and its center point was calculated with the average of the points belong to the cluster.

In this paper, the measured data from the side-view inspection are the diameter for confirming pipe type, maximum diameter and gradient of the formed part of pipes, eccentricity, etc. The equation for finding the average diameter of the pipe is as follow.

$$D_{average} = \frac{1}{n}\sum_{i=1}^{n}(P_{ui} - P_{di}) \qquad (1)$$

Fig. 3 shows the line-scanning method proposed in this paper.

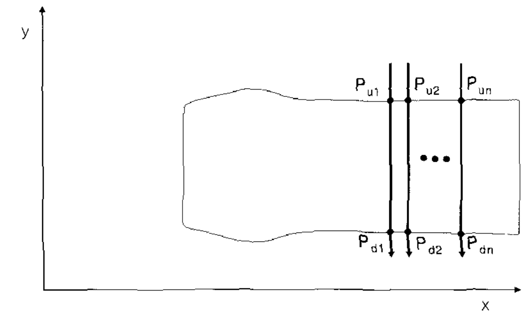

Fig.3 Measuring diameter for pipe classification using line scanning method

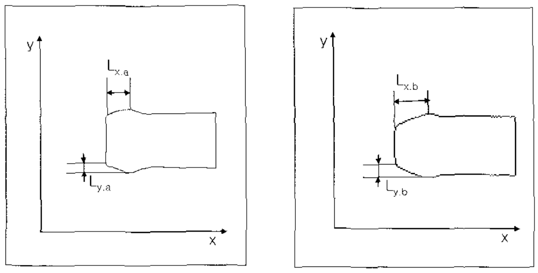

(a) φ6.35A (b) φ6.35B

Fig.4 Two types of forming shapes with same diameter

In the case of diameter *Φ6.35* pipes, there are two types of *Φ6.35* pipes according to different forming shape, as shown in Fig. 4. However, each of them can be classified by differences in length, inner diameter and maximum diameter. If both $|L_{y,a} - L_{y,b}| \ge 1.00mm$ and $|L_{x,a} - L_{x,b}| \ge 1.60mm$ are satisfied, the pipe is classified as a type A. In order to find the line equations describing the slopes of formed area, as shown in Fig.5, the Hough transform with clustering technique is applied.

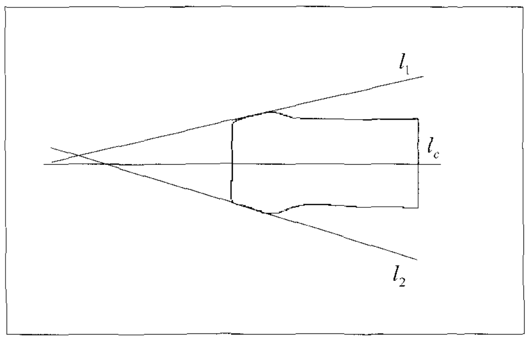

Fig. 5 Slope detection using Hough transformation

Since the gradient of the line for the normal pipes is known as $\pm 28°$, the range of gradient is divided by ten: $0.5°$ interval from $+26°$

to *+31°* , likewise *0.5°* interval from *-26°* to *-31°*. Hence, the total *20* parametric spaces are selected to be processed.

As shown in Fig.5, the line l_1 and l_2 describe the gradient values of formed area, and l_c represents the line passing through the center of the pipe. If we define point C as the intersection point made from two lines l_1 and l_2 and l_c as a line satisfying the equation of $\alpha x + \beta y + \gamma = 0$, the eccentricity e can be defined as the off-set displacement from the intersection point to l_c, as expressed in Eq. (2).

$$e = \frac{|\alpha x_c + \beta y_c + \gamma|}{\sqrt{\alpha^2 + \beta^2}} \tag{2}$$

Then, Eq. (2) can be approximated as follows.

$$y = \frac{-\alpha x - \gamma}{\beta} = y_v \qquad e = |y_c - y_v| \tag{3}$$

,where y_c is the y-coordinate value of point C, and y_v is the y-coordinate value of line l_c. The maximum diameter of the pipe is calculated by averaging the maximum valued diameter and two other values apart from 2 *Pixels* left and right side from it. In fact the image displayed on the monitor is magnified by ten times than that of the real image, so it is reasonable to make average the values of interested position and its neighbors in order to decrease the uncertainty from noise data. The maximum diameter value can be calculated by the following equation:

$$D_{\max} = \frac{1}{n}\sum_{i=1}^{n}(P_{ui} - P_{di}) \tag{4}$$

Fig. 6 shows the scanning method to find the maximum diameter.

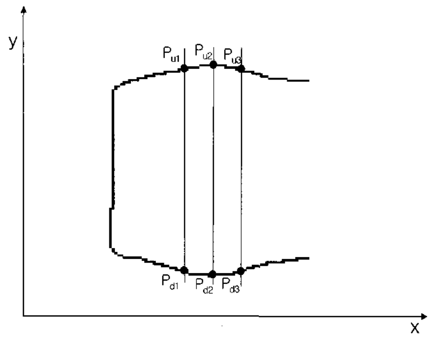

Fig. 6 Scanning method to find the maximum diameter

2.2 Front-view inspection algorithm

Using the Hough transform is time-consuming in calculation and has difficulty in detecting exact circle due to noises caused by light source. In this paper, to find the center of circle, via front-view inspection of pipe, a line scanning method is proposed.

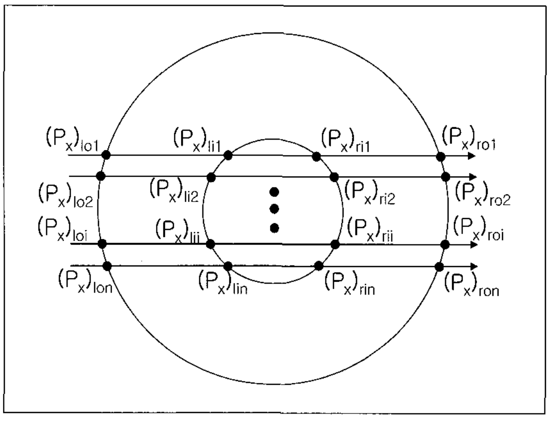

Fig. 7 Scanning method to find the center of circle

Using proper number of scanning lines into x and y direction, x and y-coordinate value of the circle can be calculated effectively. Fig. 7 shows how to find x coordinate value of the circle center. Center position and radius are averaged among their values from scanning lines in order to increase the measuring accuracy. The coordinates of the center positions can be calculated by the following equations:

$$X_{center} = \frac{1}{n}\sum_{i=1}^{n}\left[\frac{(P_x)_{loi} + (P_x)_{roi}}{2}\right] \tag{5}$$

$$x_{center} = \frac{1}{n}\sum_{i=1}^{n}\left[\frac{(P_x)_{lii} + (P_x)_{rii}}{2}\right] \tag{6}$$

$$Y_{center} = \frac{1}{n}\sum_{i=1}^{n}\left[\frac{(P_y)_{uoi} + (P_y)_{boi}}{2}\right] \tag{7}$$

$$y_{center} = \frac{1}{n}\sum_{i=1}^{n}\left[\frac{(P_y)_{uii} + (P_y)_{bii}}{2}\right] \tag{8}$$

Then, the eccentricities in the x and y direction, δ_x, δ_y, and the radii of inner and outer circle, $R_{xo}, R_{xi}, R_{yo}, R_{yi}$, can be expressed as follows:

$$\delta_x = |X_{center} - x_{center}| \tag{9}$$

$$\delta_y = |Y_{center} - y_{center}| \tag{10}$$

$$R_{xo} = \max\{(X_{center} - (P_x)_{lon}), ((P_x)_{ron} - X_{center})\} \quad n = 1, \Lambda, 100 \tag{11}$$

$$R_{yo} = \max\{(Y_{center} - (P_y)_{uon}), ((P_y)_{bon} - Y_{center})\} \quad n = 1, \Lambda, 100 \tag{12}$$

$$R_{xi} = \max\{(x_{center} - (P_x)_{lin}), ((P_x)_{rin} - x_{center})\} \quad n = 1, \Lambda, 100 \tag{13}$$

$$R_{yi} = \max\{(y_{center} - (P_y)_{uin}), ((P_y)_{bin} - y_{center})\} \quad n = 1, \Lambda, 100 \tag{14}$$

It is assumed that if the R_x, the radius in x direction, is decreased due to a forming failure, then R_y is increased. First, the larger one between left and right radius is chosen, then the smaller one between average of *3* radii in x direction and average of *3* radii in *y*-direction is taken. If a x-directional radius is larger than that of normal product because of noise evoked in *x*-direction, then *y*-directional radius is chosen, and vice versa. But that case is determined as a failure because *y*-directional radius increases by the amount of decreased *x*-directional radius.

3. Experiment for pipe-fault-detection

Using the images taken from front and side-view profiles and proposed algorithm, outer diameter, inner diameter, angle, and eccentricity are calculated, and from which a normal or faulty condition for the pipe is determined. After taking samples from normal and abnormal pipes, some experiments for reliability confirmation are conducted. Table 1 shows the criteria to determine whether the tested is normal or faulty.

Table 1 Parameter criteria for normal pipes

Pipe Type		Criterion			
Diameter (*mm*)	사두 (*mm*)	Outer Diameter (*mm*)	Inner Diameter (*mm*)	Angle (°)	Eccentricity (*mm*)
Φ6.35A	2.8	7.40±0.3	6.10±0.3	28±0.2	0.32이내
Φ6.35B	3.5	7.30±0.3	4.30±0.3	28±0.2	0.32이내
Φ8	2.8	9.30±0.3	7.90±0.3	28±0.2	0.32이내
Φ10	2.8	11.65±0.15	10.0±0.3	28±0.2	0.32이내

In order to apply the rules in Table.1, a real length per unit pixel has to be found. Therefore, it is necessary to keep the off-set distances constant among the front-view and side-view cameras and pipe. In this paper, the length per unit pixel is set up as *0.032mm/pixel*.

3.1 Side-view inspection of pipe

Fig. 8 shows straight lines that are developed by using the proposed algorithm, where we can find the angle, eccentricity, and the diameter of the pipe. Table 2 shows the coordinate values of the intersection point of two sloped lines, center position, and the eccentricity of the pipe for the case.

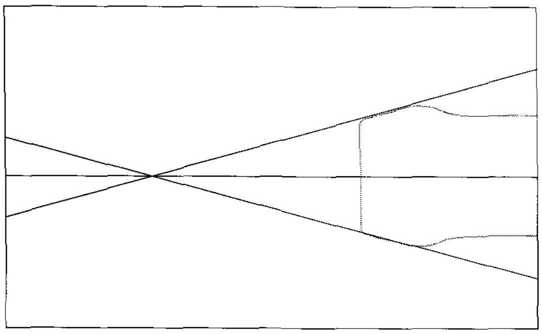

Fig. 8 Image processing result using side-view inspection algorithm

Table 2 Eccentricity from side-view inspection

Intersection Point (*Pixel*)	Center Point (*Pixel*)	Eccentricity (*Pixel*)
295	291	4

This experimental example shows that the eccentricity between intersection point and center point is about *4 pixels*. Therefore, the tested pipe can be determined as a good condition because the eccentricity of the pipe is less than *10 pixels*. The *4 pixels* is *0.13mm* in real dimension.

3.2 Front-view inspection of pipe

Fig.9 shows a front-view image through preprocess and general edge detection algorithm. After applying the proposed front-view inspection algorithm, inner and outer diameter and the eccentricity between the two diameters can be calculated.

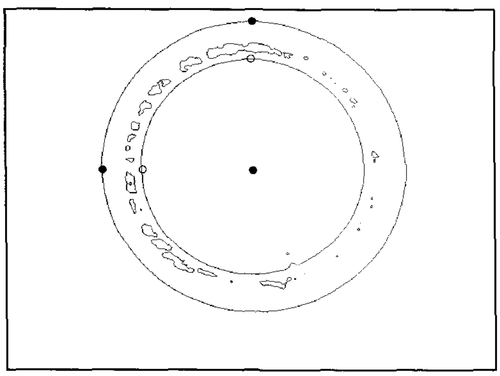

Fig. 9 Image processing result using front-view inspection algorithm

Table 3 Values of centers and radii

Content	Inner Circle (*Pixel*)	Outer Circle (*Pixel*)
x-coordinate of center	331	332
y-coordinate of center	169	171
Radius of *x*-direction	121	145
Radius of *y*-direction	124	149

Table 3 shows the center positions of inner and outer circles, and the radius of the tested pipe. The radii in the x-direction for inner and outer circles are converted into 7.74 mm and 9.28 mm, respectively. Likewise, the radii in the y direction for inner and outer circles are 7.94 mm and 9.54 mm, respectively. This information says that the tested pipe belongs to a pipe with Φ8.

3.3 Forming failure inspection of pipe

In order to test the performance of the proposed failure-inspection algorithm, two CCD cameras with *x2* magnifying lenses and *5mm* extension ring are used. Ring-type light sources are attached on the CCD cameras for better image, and also rectangular light sources were attached near the pipe to give a side-view image. *3* types of faulty pipes with *6.35mm* diameter are used to to test the performance of the algorithm as follows:

(Type A) Inner and/or outer diameter, maximum diameter failure : Fig. 10 shows the case of faulty pipe with wrong inner and outer diameters.
(Type B) Angle and/or eccentricity failure: Fig. 11 shows the case of faulty pipe with wrong angle and eccentricity due to cutting failure.
(Type C) Inner, outer, maximum diameter, angle, eccentricity failure: Fig. 12 shows the case of faulty pipe that is sent to the inspection system without completing forming. And that is the most popular case of faulty pipes. Table 1 shows the criteria for classifying normal or faulty pipe.

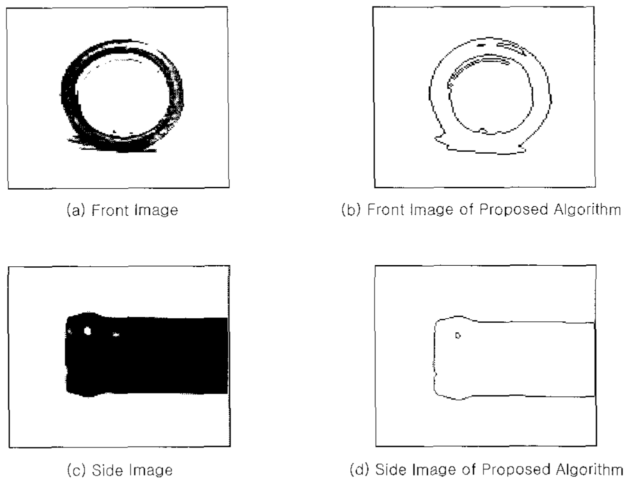

Fig. 10 Processed image of type A faulty pipe

Table 4 Inspection result of type-A faulty pipe

Inner Diameter (mm)	Outer Diameter (mm)	Angle (°)	Maximum Diameter (mm)	Eccentricity (mm)
6.92	8.11	28	8.19	0.13

Fig. 10 shows the processed image of type-A faulty pipe. The normal conditions for the pipe are as follows: the measured inner diameter of the pipe must be in the range from *5.80mm* to *6.40mm*, and all outer diameter including the maximum diameter should be between *7.10mm* and *7.70mm*. However, as shown in Table 4, all the dimension data of the tested pipe exceed normal boundary: *6.92mm* inner diameter, *8.11mm* outer diameter, and *8.19mm* maximum diameter.

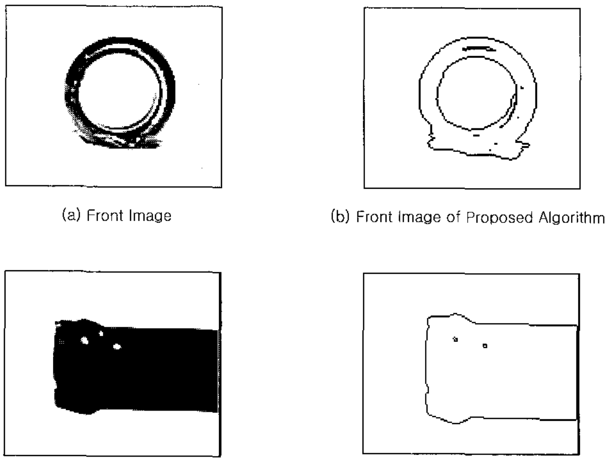

(a) Front Image (b) Front Image of Proposed Algorithm

(c) Side Image (d) Side Image of Proposed Algorithm

Fig. 11 Processed image of type B faulty pipe

Table 5 Inspection result of type-B faulty pipe

Inner Diameter (mm)	Outer Diameter (mm)	Angle (°)	Maximum Diameter (mm)	Eccentricity (mm)
6.22	7.59	∞	7.62	∞

Fig. 11 shows a case that the tip of a pipe is either damaged before going into the forming machine, or the pipe is sent to the inspection system without proper forming. This case seldom happens during the real process, but it is difficult to check the failure of the pipe. As shown in Fig. 11(c) and (d) it's difficult to find the exact angle, which makes difficult to find exact eccentricity.

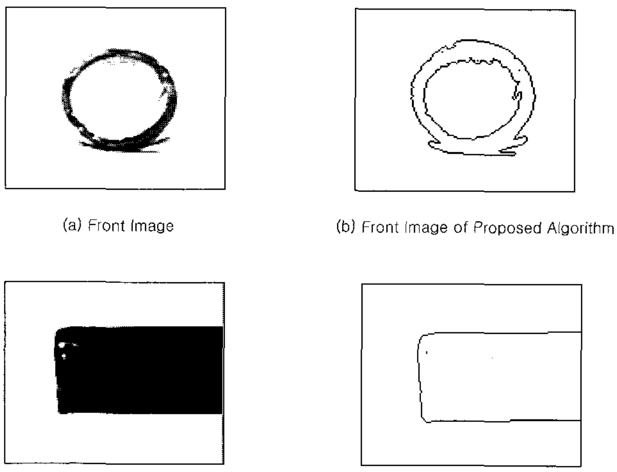

(a) Front Image (b) Front Image of Proposed Algorithm

(c) Side Image (d) Side Image of Proposed Algorithm

Fig. 12 Processed image of type C faulty pipe

Table 6 Inspection result of type-C faulty pipe

Inner Diameter (mm)	Outer Diameter (mm)	Angle (°)	Maximum Diameter (mm)	Eccentricity (mm)
5.28	6.42	∞	6.46	∞

Fig. 12 shows a case that a pipe was formed before it is completely inserted into the forging machine. This kind of pipe has a variety of forming shape and doesn't meet the dimension limit for normal forming. As shown in Table 6 inner diameter *5.28mm* deviates from the range *5.80mm ~ 6.40mm*. Outer diameter and maximum diameter are out of the proper range, and pipe angle and eccentricity are not measurable.

4. Conclusions

In this paper we developed a vision-based fault inspection system and algorithm that can inspect all pipes coming from forging machine. The system determines whether the pipe is normal or abnormal, and the faulty pipe is discarded by a removing actuator. At the same time the inspection result data, data and image files, are delivered to the server computer. A modified Hough transform and line scanning method are used to analyze the pre-processed image, and from which the status of the pipe is determined to be good or faulty.

The forging machine takes about 1 sec to draw the pipe, form and release the pipe. That means the whole inspection time should be accomplished in a second. The inspection system spends about 720 *ms* to finish the inspection process including the signaling time from/to the main controller. Therefore, the developed inspection system satisfies the required time. Also, a data overflow problem with stack of data and image files, is solved.

In general, the pipes produced in the plant have 4/100mm of eccentricity. Sometimes this can cause a problem to determine the fault status. Since the inspection system can guarantee the accuracy of 0.01 mm, it can remove the decision error from the pipe irregularity. Therefore, it is concluded that the developed inspection can be successfully applied to the real plant system and satisfies the all requirements.

ACKNOWLEDGEMENT

This work was supported by 2002 Research Fund of University of Ulsan.

REFERENCES

1. Otsu, N., "A Threshold seleciton Method from Gray Level Histograms," IEEE Trans. Syst. Man Cybernet., Vol. SMC-9, pp. 62-66. 1979.
2. Park, H. J., Hwan, Y. M., "Dimensional Measurement Using the Machine Vision," KSPE, Vol. 18, No. 3, pp.10-17, 2001.
3. Maitre, H., "Contribution to the prediction of prediction of performance of the Hough transform," IEEE Trans. On Patten Analysis and Machine Intelligence., PAMI-8. 5, 1986.
4. Braggins, D. W., "Image processing for industrial applications in Europe," Proceedings of the 5th International Conference on Robot Vision and Sensory Control. pp. 13-23
5. Persoon, E., "A Pipelied Analysis System Using Custom Integrated Circuits," IEEE On Patten Analysis and Machine Intelligence, Vol. 10. No. 1, pp. 110-116, 1988.
6. Gotoh, T., Toriu, T., Sasaki, S., "A Flexible Vision-Based Algorithm for a Book Sorting System," IEEE On Patten Analysis and Machine Intelligence, Vol. 10, No. 3, pp. 393-399, 1988.
7. Shapiro, S. D., "Transform for the Computer Detection of Curves in Noisy Picture," Comp. Gragpics Image Process. 4, pp. 328-338. 1975.
8. Ballad, D. H., "Generalizing the Hough Transform to Detect Arbitrary shapes," Pattern Recongniton, 13, pp. 111-121, 1981.
9. Leavers, V. F., "The dynamic Generalized Hough Transform," First ECCV conf. Antibes, France, 1990.
10. Califano, A., Tayler, R. W., "A new approach to complex Parameter Feature Extraction," IEEE On Patten Analysis and Machine Intelligence, pp. 192-199. 1989.